1

Next Generation of Optical Access Network Based on Reflective-SOA

Guilhem de Valicourt
Alcatel-Lucent Bell Labs France, Route de Villejust, Nozay, France

1. Introduction

Communication networks have evolved in order to fulfil the growing demand of our bandwidth-hungry world. First, the coaxial cable has replaced the copper cable since 1950 for long- and medium-range communication networks. The Bit rate-distance product (BL) is commonly used as figure of merit for communication systems, where the B is the bit rate (bit/sec) and L is the repeater spacing (km). A suitable medium for transmission needed to be available and optical fibres were selected as the best option to guide the light (Kao & Hockham, 1966). A radical change occurred, the information was transmitted using pulses of light. Thus further increase in the BL product was possible using this new transmission medium because the physical mechanisms of the frequency-dependent losses are different for copper and optical fibres. The bit-rate was increased in the core network by the introduction of a new technique: Wavelength-Division Multiplexing (WDM). The use of WDM revolutionized the system capacity since 1992 and in 1996, they were used in the Atlantic and Pacific fibre optic cables (Otani et al., 1995).
While WDM techniques were mostly used in long-haul systems employing EDFA for online amplification, access networks were using more and more bandwidth. Access network includes the infrastructures used to connect the end users (Optical Network Unit - ONU) to one central office (CO). The CO is connected to the metropolitan or core network. The distance between the two network units is up to 20 km. The evolution of access network was very different from in the core network. High bit-rate transmissions are a recent need. At the beginning, it provided a maximum bandwidth of 3 kHz (digitised at 64 kbit/s) for voice transmission and was based on copper cable. Today, a wide range of services need to be carried by our access network and new technologies are introduced which allow flexible and high bandwidth connection. The access network evolution is obvious in Europe with the rapid growth of xDSL technologies (DSL: Digital Subscriber Loop). They enable a broadband connection over a copper cable and allow maintaining the telephone service for that user. In 2000, the maximum bit rate was around 512 kbit/s while today it is around 12 Mbit/s. However since 2005, new applications as video-on-demand need even more bandwidth and the xDSL technologies have reached their limits. The introduction of broadband access network based on FTTx (Fiber To The x) technology is necessary to answer to the recent explosive growth of the internet. Today, Internet service providers propose 100 Mbit/s using optical fibre. The experience from the core network evolution is a great benefit to access network. The use of WDM mature technology in access and

metropolitan network should offer more scalability and flexibility for the next generation of optical access network.
However the cost mainly drives the deployment of access network and remains the principal issue. Cost effective migration is needed and the cost capital expenditures (CAPEX) per customer has to be reduced. ONU directly impacts on the CAPEX. New optical devices are needed in order to obtain high performances and low cost ONU.
For uplink transmission systems using WDM, each ONU requires an optical source, such as a directly modulated laser (DML) (Lelarge et al., 2010). If wavelengths are to be dynamically allocated, one to each ONU, colourless devices are needed in order to minimize the deployment cost. Reflective Semiconductor Optical Amplifier (RSOA) devices can be used as a low-cost solution due to their wide optical bandwidth. The same type of RSOA can be used at different ONUs where they perform modulation and amplification functions. However, cost and compatibility with existing TDM-PONs is still an issue. As a consequence, hybrid (TDM+WDM) architecture is being investigated for next generation access network (An et al., 2004), as a transition from TDM to WDM PONs where some optical splitters could be re-used. Recently, the first commercial hybrid PON based on reflective semiconductor optical amplifiers (RSOA) has been announced (Lee H-H. et al., 2009). Such a network allows serving 1024 subscribers at 1.25 Gbit/s over 20 km.
In this chapter, the basic theory of SOA/RSOA is investigated. The different interactions of light and matter are described. Then, we focus on the device modelling. We develop a multi-section model in order to take in account the non-homogeneity of the carrier density. In this approach, we consider a forward and backward propagation as well as the amplified spontaneous emission (ASE) propagation. Longitudinal spatial hole burning (LSHB) strongly affects the average optical gain. An evaluation of the total gain in RSOA devices including the LSHB is proposed. The influence of the optical confinement and the length is described and leads to some design rules. Under the latter analysis, the performance of RSOA must be evaluated considering the trade-offs among the different parameters.
Dynamic analysis is then proposed in section 4. The RSOA modulation responses behave as a low-pass filter with a characteristic cut-off frequency. The carrier lifetime turns out to be a key parameter for high speed modulation and a decrease of its value appears to be required. The rates of recombination processes, such as stimulated, spontaneous and non-radiative recombination govern the carrier lifetime. They strongly depend on the position along the active zone and the operating conditions.
Furthermore, telecommunication networks based on RSOA are studied. We introduce the envisaged architectures of access networks based on RSOA. High gain RSOA is used as colourless transmitter and WDM operations are performed. Laser seeding configuration at 2.5 Gbit/s is realized and error free transmission is obtained for 36 dB of optical budget over 45 km of SMF. Low-chirp RSOAs enable a 100 km transmission at the same bit rate below the Forward Error Correction (FEC) limit. Direct 10 Gbit/s modulation is then realized using high speed RSOA.
Finally, we summarize the lessons learned in this chapter and conclude on RSOA devices as colourless optical transmitters.

2. Past history and basic concept of reflective SOA

In this section, the fundamental properties and the main concepts of SOA and RSOA are introduced in a simple way. We discuss the past history and the evolution of RSOA with the

development of optical communication systems. Then, we detail the physics involved in SOA and RSOA. A multi-section approach is chosen to model the device behaviour under static conditions. The aim of this section is not to propose a complex model but to underline and understand the different mechanisms in RSOA devices.

2.1 RSOA evolution

The first idea of a Reflective SOA (RSOA) was proposed by Olsson in 1988 to reduce the polarization sensitivity via a double pass configuration using classic SOA.
The first integrated RSOA for optical communication appeared in 1996 where the device was employed for upstream signal modulation at a bit rate of 100 Mbit/s (Feuer et al., 1996). Then several experiments based on RSOAs for local access network were realized where the bit rate was increased to 155 Mbit/s (Buldawoo et al, 1997).
In this chapter, we mainly focus on the wavelength upgrade scenario for WDM-PON systems. While current optical access networks use one single upstream channel to transmit information, WDM systems use up to 32 channels increasing therefore the total transmitted information. RSOA is the perfect candidate because of its wide optical bandwidth, large gain and low cost, therefore fulfilling most of the requirements. For instance, its large optical bandwidth makes it a colourless cost-effective modulator for WDM-PON. The same type of device can be used in different ONUs, which reduces the network cost. Moreover, the large gain provided by an RSOA can compensate link losses without using an extra amplifier, which simplifies the overall solution.
Therefore since 2000, RSOA devices saw a fast growing interest in upstream channels transmission based on reflective ONU for WDM-PON applications. The first re-modulation scheme has been proposed in 2004 where the downlink signal was transmitted at 2.5 Gbit/s and uplink data stream was re-modulated on the same wavelength via the RSOA at 900 Mbit/s (Koponen et al, 2004). Then further investigations were realized and 1.25 Gbit/s re-modulation was demonstrated (Prat et al., 2005).
Today, several research groups work on these solutions such as Alcatel-Lucent Bell Labs, III-V Lab, Universitat Politècnica de Catalunya (UPC), Orange labs, ETRI, KAIST, IT and various optical devices manufacturers proposed commercial RSOA devices as CIP, MEL and Kamelian.

2.2 Fundamentals of SOA and RSOA

Gain in a semiconductor material results from current injection into the PIN structure. The relationship between the current I and the carrier density (n) is given by the rate-equation. The rate-equation should include the stimulated emission as well as the spontaneous and absorption rate. R(n) is the rate of carrier recombination including the spontaneous emission and excluding the stimulated emission. Electrons can recombine radiatively and non-radiatively therefore R(n) can be written as:

$$R(n) = R_{rad}(n) + R_{non-rad}(n) \quad (1)$$

When an electron from the Conduction Band (CB) recombines with a Valence Band (VB) hole and this process leads to the emission of a photon, it is called the radiative recombination. The rate of radiative recombination is:

$$\mathrm{R_{rad}(n)} = \mathrm{B.n^2} \quad (2)$$

This term corresponds to the spontaneous emission recombination. Non-radiative processes deplete the carrier density population in the CB then fewer carriers remain available for the stimulated emission and the generated amount of light is limited. The three main non-radiative recombination mechanisms in semiconductor are:

- The linear recombination due to the transfer of the electron energy to the thermal energy (in the form of phonons). This mechanism is called the Shockley-Read-Hall (SHR) recombination. The rate of SRH recombination is:

$$R_{SRH} = A.n \tag{3}$$

- The Auger recombination due to the transfer of the energy from high-energy electron/hole to the low-energy electron/hole with subsequent energy transfer to the crystal lattice. The rate of the Auger transitions is:

$$R_{Aug} = C.n^3 \tag{4}$$

- Another non-radiative recombination process is the carrier leakage, where carriers leak across the SOA heterojunctions. The leakage rate depends on the drift or the diffusion of the carriers therefore is given by (Olshansky et al., 1984):

$$R_{leak} = D_{leak}.n^{3.5} \text{for diffusion and } R_{leak} = D_{leak}.n^{5.5} \text{ for drift} \tag{5}$$

The dominant leakage current is usually due to carrier drift. Therefore the total recombination rate is given by:

$$R(n) = R_{rad}(n) + R_{non-rad}(n) = A.n + B.n^2 + C.n^3 + D_{leak}.n^{5.5} \tag{6}$$

The carrier leakage is usually neglected. So the rate-equation states that the resulting change of the carrier density in the active zone is equal to the difference between the carrier supplied by electrical injection and the carrier's recombination. Amplification results from stimulated recombination of the electrons and holes due to the presence of photons. The interaction between photons and electrons inside the active region depends on the position and the time. Therefore the carrier density at z and t is governed by the final rate-equation. We neglect carrier diffusion in order to simplify the carrier density rate-equation. This assumption is valid as long as the amplifier length L is much longer than the diffusion length, which is typically on the order of microns. We also assume that the carrier density is independent of the lateral dimensions.

$$\frac{dn(z,t)}{dt} = \frac{I(t)}{e.V} - (A.n(z,t) + B.n(z,t)^2 + C.n(z,t)^3) - v_g g_{net}.S(z,t) \tag{7}$$

Where n(z,t) is the carrier density, I(t) is the applied bias current, S(z,t) is the photon density, g_{net} is the net gain and vg is the light velocity group.

A time domain model for reflective semiconductor optical amplifiers (RSOAs) was developed based on the carrier rate and wave propagation equations. The non linear gain saturation and the amplified spontaneous emission have been considered and implemented together in a current injected RSOA model (Liu et al., 2011). This approach follows the same analytical formalism as Connelly's static model (Connelly, 2007).

To make the model suitable for static analysis some assumptions have been made and simplifications have been introduced. Since, as a modulator, the RSOA is mainly illuminated by a CW optical source, the material gain is assumed to vary linearly with the carrier density

but with no wavelength dependence. Amplified spontaneous emission power noise is assumed to be a white noise, with an equivalent optical noise bandwidth. When the current is modulated in a RSOA, the carrier density and the photon density are varying with time and position. This is caused by the optical wave propagation and the carrier/photon interaction. The carrier density variation is introduced in the model by dividing the total device length into smaller sections. For each section the carrier density is assumed to remain constant along the longitudinal direction. The equations are linking the driving current, the carrier density and the photon density. Figure 1 represents the model elementary section. It includes ports representing the input and output photon density (forward and backward), input and output amplified spontaneous emission (forward and backward), the input electrical current injection and carrier density. We do not consider the phase shift of the signal.

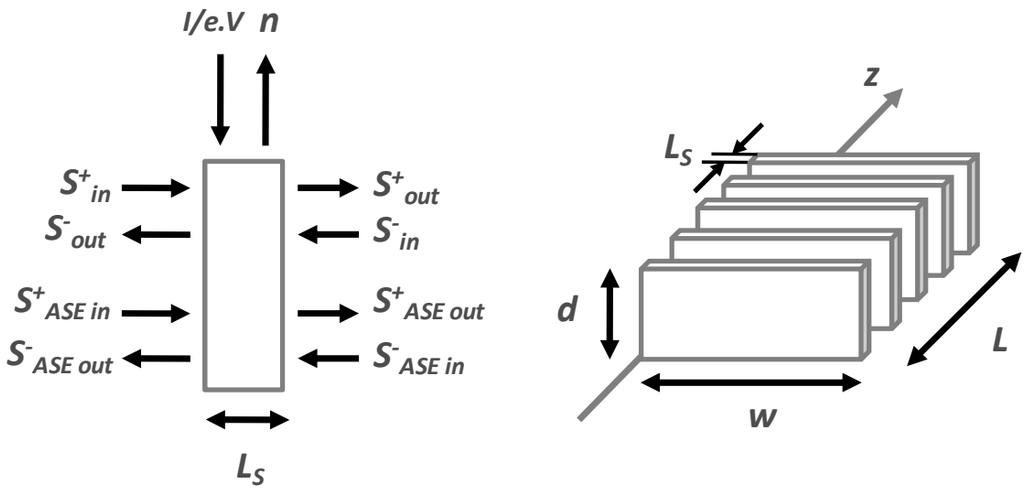

Fig. 1. RSOA elementary representation for numerical modelling

The forward and backward propagating optical fields (excluding spontaneous emission) are described by the relation between the input optical power and output optical power.

$$P^{\pm}(z \pm \Delta z) = P^{\pm}(z)e^{g_{net}\Delta z} \tag{8}$$

The material gain (g_m) is usually approximated by a linear function of the carrier density. In general the material gain also depends on the photon density S. For high photon density, the gain saturates and this phenomenon is described by the gain compression factor. Then, the material gain equation becomes:

$$g_S = \frac{g_m}{1+\varepsilon.S} \tag{9}$$

Where ε is the gain saturation parameter.
The boundary conditions for the device input and output facets, are given by:

$$\begin{aligned} P^{+}(0) &= (1 - R_1)P_{in} + R_1P^{-}(0) \\ P^{-}(L) &= R_2P^{+}(L) \end{aligned} \tag{10}$$

Where R_1 and R_2 are power reflection coefficients.

The amplified spontaneous emission is the main noise source in an RSOA and determines the RSOA static and dynamic performances under low input optical power. For high stimulated emission output power the spontaneous emission drops significantly and its impact on the device performances is less significant. For a section of length Δz the ASE power spectral density generated within that section is given by the following equation :

$$\mathrm{P_{ASE}} = \eta_{Sp}(G_S(\mathrm{z}) - 1)\mathrm{h\nu B_0} \tag{11}$$

Where G_s is the single pass gain of one section and η_{sp} is the spontaneous emission factor. The spontaneous emission factor can be approximated by (D'Alessandro et al., 2011):

$$\eta_{Sp} = \frac{n}{n - \mathrm{n_0}} \tag{12}$$

In our model we have assumed a constant noise power spectral density over an optical bandwidth B_o. The bandwidth B_o is estimated at 5x10^{12} Hz. The implementation of the ASE noise travelling wave follows a procedure similar to the optical signal travelling wave. The spontaneous emission output power for the forward and backward noise signals has two contributions: the amplified input noise and the generated spontaneous emission component within the section. The gain variations with the bias current (Experimental and modelled) are compared in Figure 2.

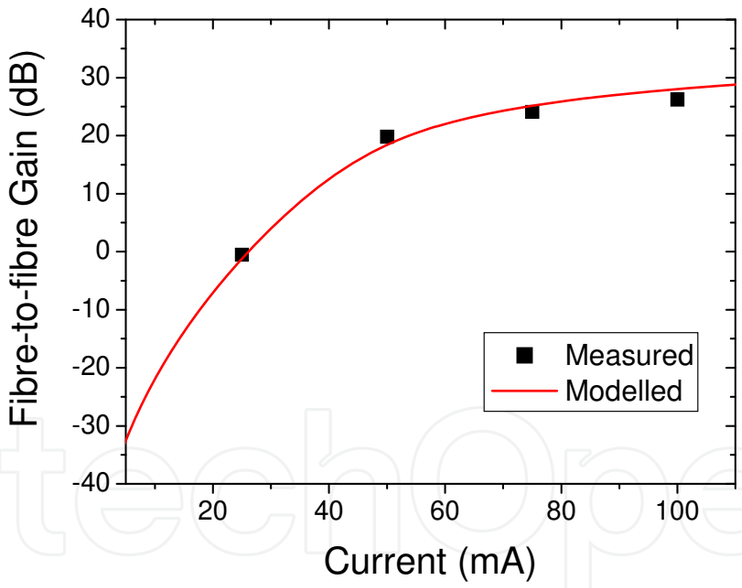

Fig. 2. Fibre-to-fibre gain for RSOA versus bias current

The carrier density profile is represented in figure 3 as well as the total photon density. At low input injection (P_{in} = -40 dBm), the carrier density profile is in this case not symmetrical due to the high reflection of the second facet. Strong depletion occurs from the ASE and the signal double propagation (reflective behaviour of the device). Also at P_{in} = -40 dBm, the ASE power dominates the signal power which explains that the RSOA device saturates more at high input electrical current.

At high input optical power, the carrier density in an RSOA is flattened due to the forward and backward propagations of the signal inside the device. The saturation effect occurs all

along the RSOA. At the mirror and input facets, the signal photon density becomes larger with the injected current as it has been more amplified during the forward and backward propagations.

From this preliminary analysis, a general conclusion can be deduced. RSOAs should saturate faster than classic SOAs. The overall photon density inside a RSOA is larger than in a classic SOA, reducing the material gain available for signal amplification. However the forward and backward signal amplifications could compensate for this effect. Large photon density should also affect the E/O bandwidth and could be useful to obtain high speed devices. All these effects are stronger at high input electrical injection and high input optical power.

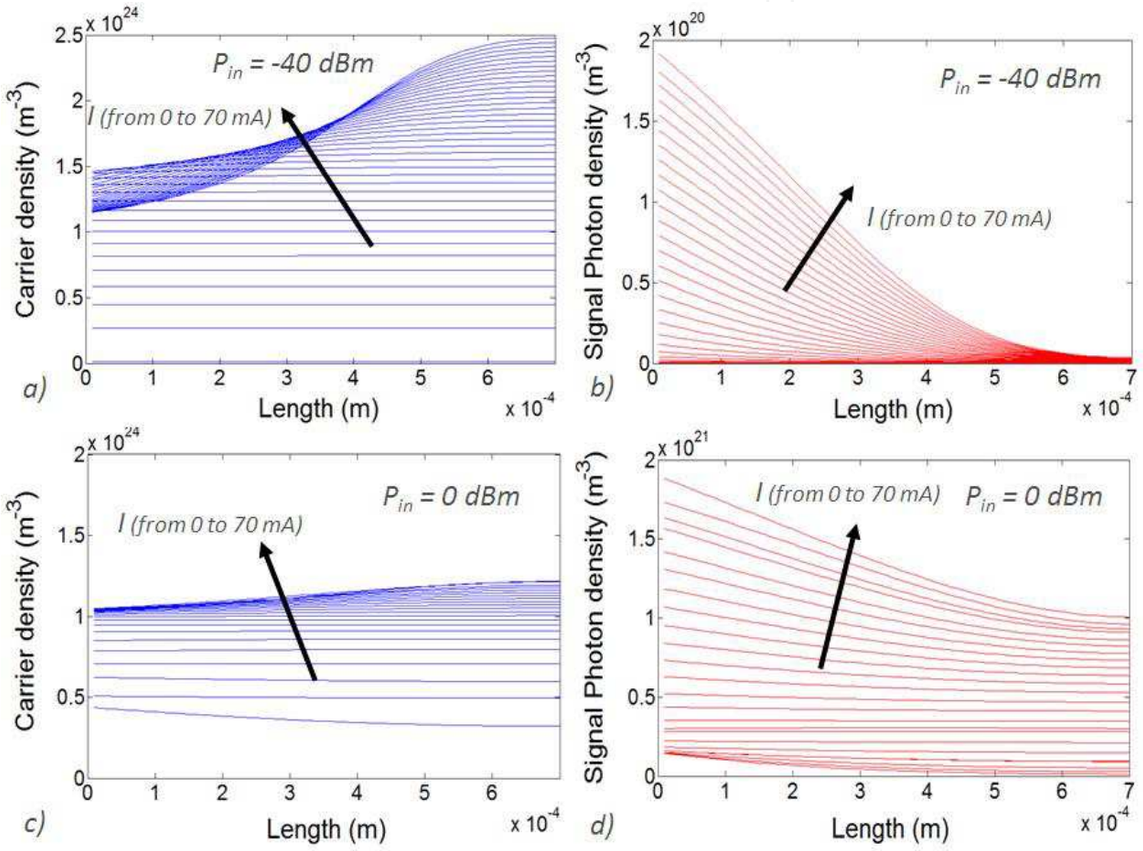

Fig. 3. Carrier and photon density spatial distribution in RSOA device. (a) and (b) represents the simulation from Pin = -40 dBm ; (c) and (d) for 0 dBm

3. RSOA devices static characteristics

Optical gain measurements depending on the input current and optical power were realized. Figure 4 shows the experimental setup which is used to perform static measurements. The required wavelength controlled by an external cavity laser is launched into the RSOA through an optical circulator (OC). A combined power meter and attenuator is used to control the input power to the RSOA. An optical spectrum analyser and a power

meter are used in order to determine the static performances of the device, such as optical gain, gain peak, bandwidth and ripple, noise figure and output saturation power. The impacts of these several parameters (Γ and L) are experimentally studied in the next sub-sections.

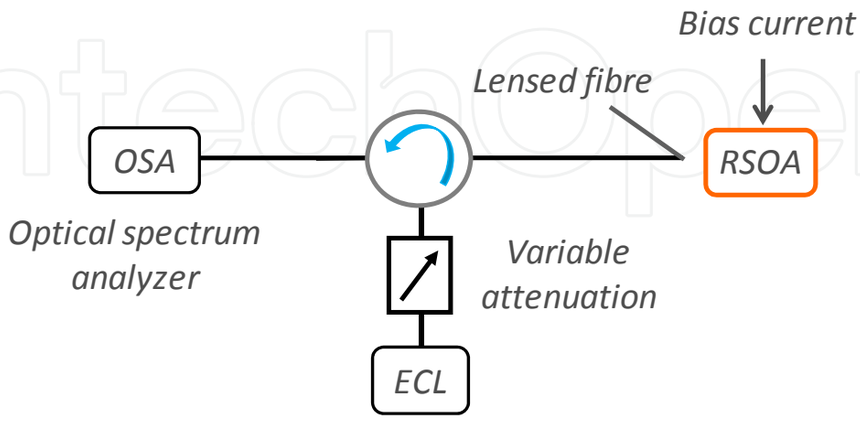

Fig. 4. Static experimental setup

3.1 Influence of the optical confinement

The optical gain for the optical confinements of Γ~20% and Γ~80% are compared depending on the input electrical current and optical power in Figure 5. The gain increases with the bias current as modelled in previous section and starts to saturate at high electrical injection. The low confinement factor (Γ~20%) devices show higher gain than the high confinement factor (Γ~80%) devices. This result is counter-intuitive as the net gain should increase with higher optical confinement and therefore the single pass gain. High Γ means more ASE and more saturation. Thus a low confinement factor induces lower spontaneous emission power by reducing the effect of the ASE inside the device (Brenot et al., 2005). As the RSOA is less saturated, the single pass gain is also increasing with the reduced confinement factor (because the LSHB is reduced).We demonstrated that RSOA devices have a non-uniform carrier density along the active zone. This interpretation can be confirmed by the simulations of the carrier density spatial distribution (section 2) and SE measurements (section 3.2).

Increasing the input power, the gain drops quickly due to the saturation effect. That is, the increase of optical input power at a constant current consumes many carriers for the stimulated emission therefore decreases the carrier density and increases the saturation effect. This transition corresponds to the frontier between the linear and the saturated regime. In this regime, the noise factor increases due to gain saturation. A common and useful figure of merit is the dependence of the optical gain on the output power. From this curve, we obtained the saturation power (P_{sat}) when the gain drops by 3 dB. Figure 5 (b) shows the optical gain versus the output power.

Most of SOA devices show saturation power around 10 dBm and optimized SOA can reach 20 dBm (Tanaka et al., 2006). However optimizing for maximum saturation power induces low gain (<15 dB) and large energy consumption (I > 500mA). In RSOA devices, high gain is obtained as well as reasonable saturation power.

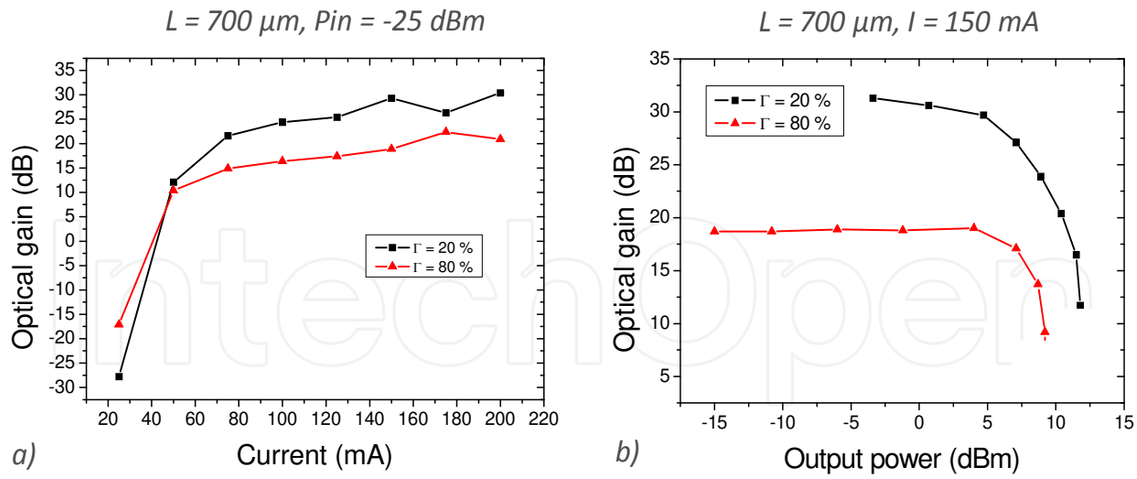

Fig. 5. Confinement effect on 700 µm long RSOA depending on the current (a) and the output power (b)

3.2 Saturation effect in long RSOA

Two optical confinement values have been studied and low optical confinement (Γ~20 %) enables the fabrication of high gain devices. It was the consequence of the LSHB reduction inside the active material which leads to an overall higher gain. However, the length (L) also affects the single pass gain (G_s). Again two effects are in competition inside the active zone: the exponential growth of G_s with the length and the non-homogenous carrier density distribution (which leads to strong saturation effect). Therefore a trade-off needs to be found in order to balance these two effects. By increasing the length, the forward and backward amplifications are also increased up to an optimum point. Devices that are too long induce high saturation and reduce the optical gain. Figure 6 (a) shows the optical gain versus the current density in different RSOA cavity lengths. The current density (J) is more relevant from a device point of view in order to compare similar operating conditions.

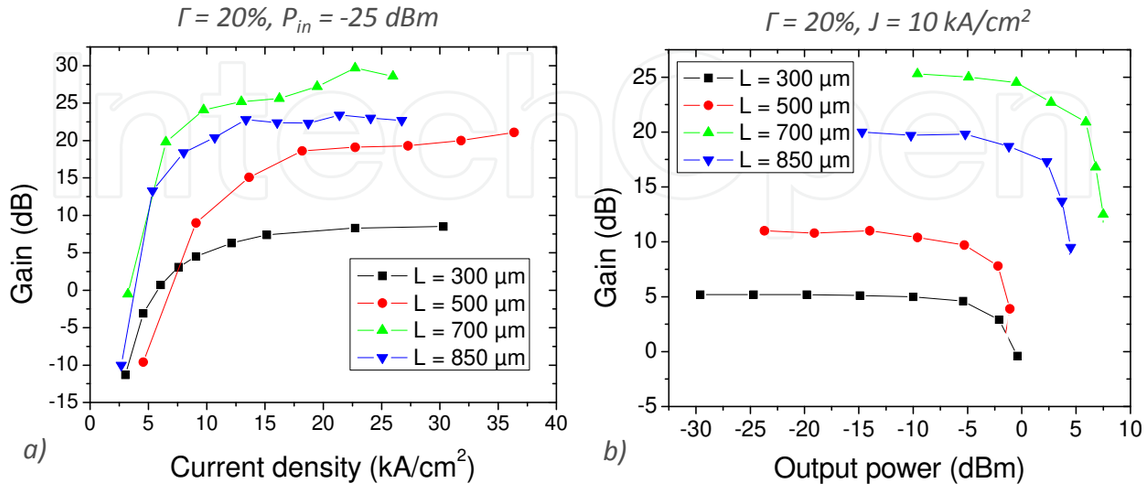

Fig. 6. Length effect on 20% optical confinement RSOA depending on the current density (a) and on the output power (b) for J = 10 kA/cm2

At first, the increase of the cavity length induces higher optical gain (from 300 µm to 700µm) however when it reaches 850 µm, the gain drops back. Therefore a maximum gain is obtained for 700 µm long devices. The optical gain versus the output power is presented in Fig. 6. (b) at the current density J = 10 kA/cm². We can notice that increasing the gain leads to higher saturation power. It can be explained by the fact that we are at a constant current density therefore the electrical bias current increases with the length of the device leading to an improvement of the saturation power. For one specific optical confinement (Γ = 20%), an optimal length can be found in order to obtain the best static performances (high optical gain). At first, the optical gain increases linearly with the length. In fact, the forward and backward amplifications control the single pass gain. Figure 7. (a) represents the SE measurements where an optical fibre is placed along the active zone at the input/output, centre and mirror region. Then SE measurements as a function of the injected current are measured. SE measurements are performed in 700 µm long RSOA in order to confirm the presence of the saturation effect.

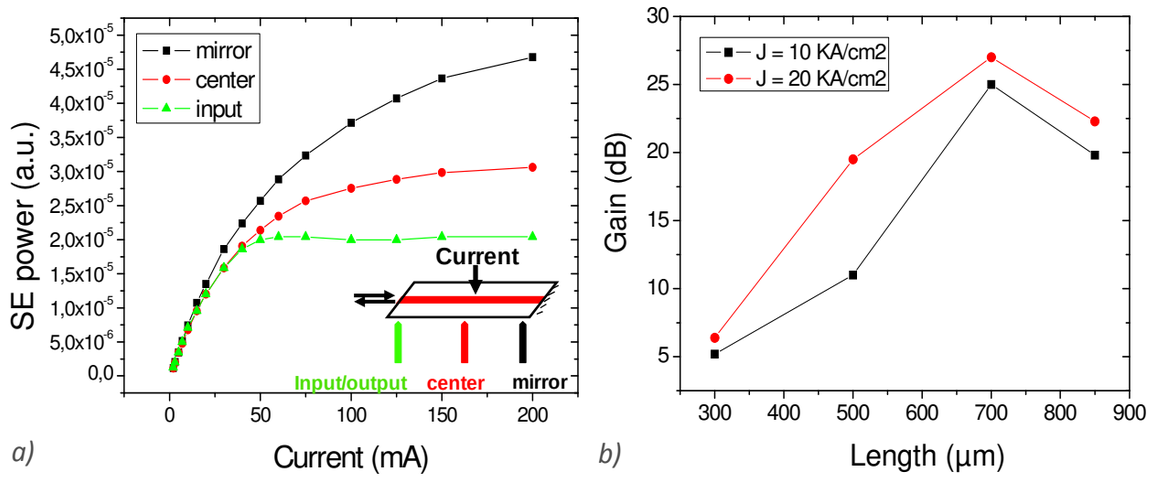

Fig. 7. (a) SE schematic and measurements; LSHB effect on (b) the optical gain in RSOA device

At low input bias current, no difference is observed due to the flat carrier density. The saturation effect starts to appear above 50 mA when the carrier density spatial distribution becomes non-homogeneous. Low SE power is collected at the input region due to the saturation effect which means low carrier density in the region. However the mirror region emits more SE power due to the high carrier density value. This demonstrates the presence of a strong saturation effect in the device.

In longer RSOAs, the depletion becomes stronger which induces a lower overall carrier density and a larger absolute difference in the carrier density between input and mirror facet. When varying the length of the RSOA, those several effects account for the existence of an optimum length where the optical gain is maximised. The optical gain versus the length of the device is plotted on Figure 7. (b) for two current densities.

4. Modulation characteristics and performances

RSOA devices have limited electro-optical (E/O) bandwidth between 1 to 2 GHz (Omella et al., 2008) compared to laser devices usually between 8 to 10 GHz. The difference can be

explained by two effects that are not present in RSOA devices. The first effect is gain clamping. The carrier density stays low even at high electrical input current while the photon density is increasing. This produces a shorter carrier lifetime particularly advantageous for high speed modulation. The second effect is the electron to photon resonance due to the presence of a cavity. The resonance appears in the modulation response increasing the effective -3dB E/O bandwidth.
The absence of cavity in RSOAs limits the modulation speed of this device. The modulation response behaves as a low pass filter with a characteristic cut-off frequency (when the link gain drops by 3dB). One limitation is due to carrier density spatial distribution. High carrier density combined with low photon density induces long carrier lifetime. Furthermore the carrier and photon densities strongly depend on the position z along the device. Therefore a non-homogeneous carrier lifetime is obtained.

4.1 Carrier lifetime analysis

The objective is to obtain a first order approximation of the carrier lifetime for the steady state condition. We can demonstrate that the carrier lifetime can be approximated by:

$$\frac{1}{\tau_{eff}} = A + B.n + C.n^2 + \Gamma \times a \times S \times v_g \tag{13}$$

Where the differential gain is defined by $a = \frac{\partial g}{\partial N}$, Γ is the optical confinement factor and S is the total photon density including the signal and the ASE.
The carrier lifetime is inversely proportional to the recombination rate. The recombination rate can be described using two different terms: one directly proportional to the spontaneous emission and non-radiative recombination (due to the defect or Auger process as described in section 2.2) and the second one depending on the stimulated recombination.

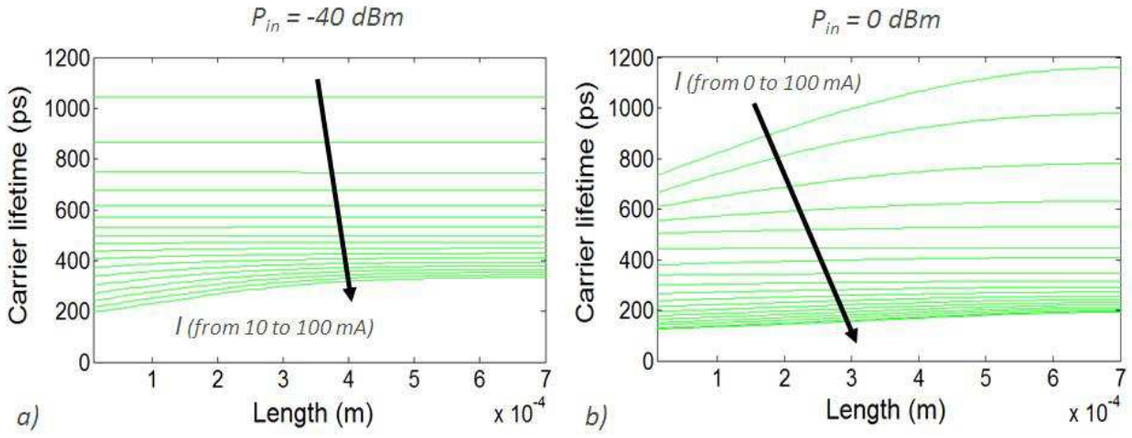

Fig. 8. Carrier lifetime simulation along 700 µm RSOA device at (a) low (Pin = -40 dBm) and (b) high (Pin = 0 dBm) optical injection

Simulations of the carrier lifetime have been carried out along the active region. Figure 8 represents the results with the bias current as parameter at P_{in} = -40 dBm (Figure 8 (a)) and Pin = 0 dBm (Figure 8 (b)). Obviously, in both cases, carrier lifetime decreases by increasing

the input electrical current. It is mainly due to the increase in all recombination terms. The second important observation is the non-uniformity of the carrier lifetime along the device. At large optical input power (P_{in} = 0 dBm), the saturation effect described in section 3.2 is much stronger than with low input injection at low bias current. The average carrier lifetime is also smaller in this condition, due to a larger photon density. In order to understand the influence of the different recombination mechanisms on the carrier lifetime, it is important to follow the evolution of the different recombination terms depending on the bias current and the input optical power.

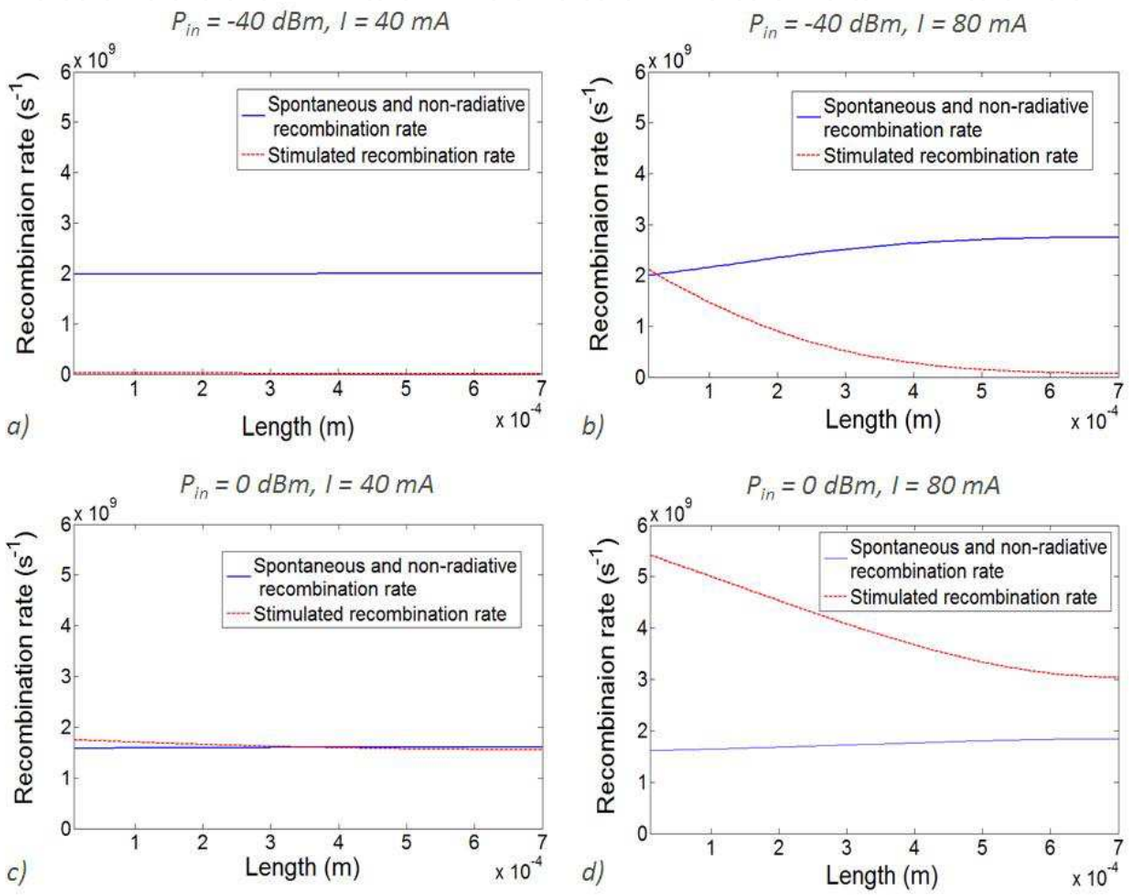

Fig. 9. Spatial distribution of spontaneous and non-radiative recombination rate compared to stimulated recombination rate in 700 µm long RSOA at different input conditions. (a) Pin = -40 dBm and I = 40 mA, (b) Pin = -40 dBm and I = 40 mA, (c) Pin = 0 dBm and I = 40 mA and (d) Pin = 0 dBm and I = 80 mA

Figure 9 represents the spatial distribution of the two terms at various operation conditions. At low input optical power ((a) and (b)), the spontaneous and non-radiative recombination rates are dominant even at high bias current. Therefore the carrier lifetime depends on this recombination term. At high input optical power ((c) and (d)), the photon density is much higher than in the previous situation, thus the stimulated recombination rate tends to overcome the spontaneous and non-radiative recombination terms. This is also confirmed at high input bias current (d) when the signal and ASE are strongly amplified along the RSOA.

However at low bias current (c), both phenomena balance each other and both are responsible for the carrier lifetime. They are more or less equal and do not vary that much over z. This analysis is crucial for digital modulation as the input conditions change over time, therefore the dynamic of the device will depend on which recombination rate is dominant at a precise time.
In order to validate our simulation, a comparison with experimental measurements should be done. High-frequency characterization is then needed. The experimental set-up and results are described in the next section.

4.2 High-frequency experimental set-up and characterization

We realize a RSOA-based microwave fibre-optic link as depicted in figure 10. All different devices of this experimental set up can be considered as two-port components and classified according to the type of signal present at the input and output ports. E/E, E/O, O/E or O/O are possible classifications where an electrical (E) signal or an optical (O) signal power are modulated at microwave frequencies (Iezekiel et al., 2000).The RSOA is considered as an E/O two-port device which is characterized by the electro-optic conversion process, i.e. the conversion of microwave current to modulated optical power.

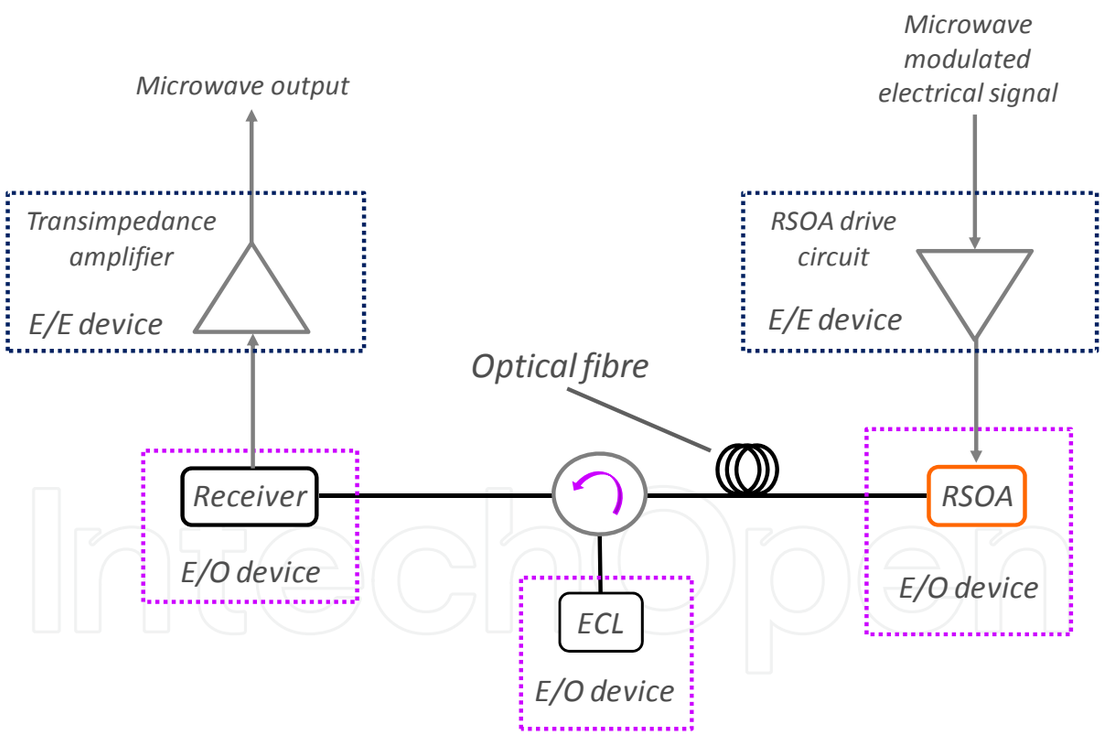

Fig. 10. High speed fibre-optic link

A full two-port optical characterisation of the complete set up is important to quantify the system performances. Dynamic characterization allows the measurement of the electrical response of the two-port network. A high-frequency signal is sent to the RSOA and the optical modulation is detected by a photodiode. The $|S_{21}|^2$ parameter (link gain) is measured over a range of frequency from 0 to 10 GHz. Figure 11 shows the electrical response of a typical RSOA device.

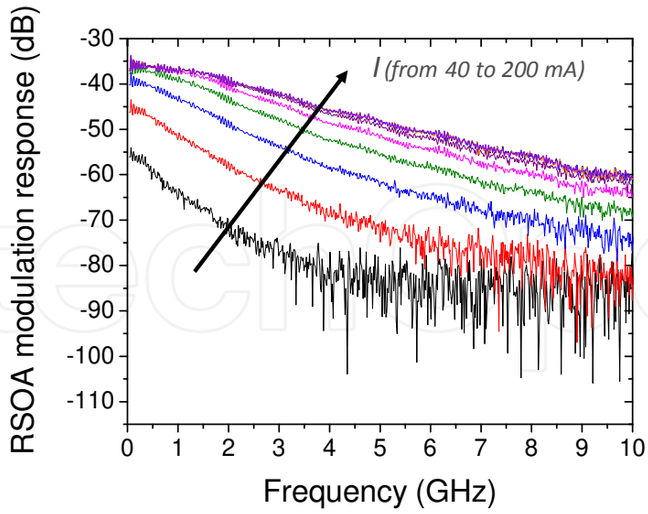

Fig. 11. Direct modulation measurements S21 in 700µm long RSOA device

We simulate the modulation bandwidth depending on the carrier lifetime based on the first order approximation. The carrier lifetime can be estimated along the RSOA but shows a non-homogenous spatial distribution. The first approach consists of considering an average carrier lifetime over the whole device. Simulation and experimental data are compared in Figure 12-(a) for a 700 µm long RSOA at 80 mA. The simulation results fit well with the measurements over a limited range (from 0 to 2GHz). The difference beyond can be explained by the addition of the buried ridge structure (BRS) limitation. In fact, the BRS equivalent electrical circuit exhibits a cut-off frequency around 3 GHz.

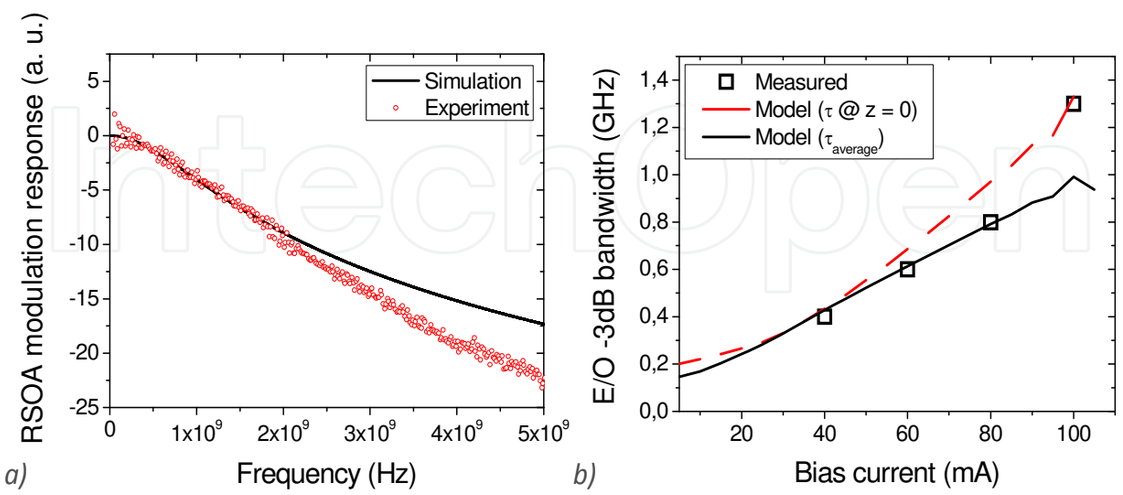

Fig. 12. RSOA (a) E/O modulation bandwidth versus frequency at I = 80 mA (b) -3 dB E/O modulation bandwidth versus bias current for 700µm of AZ

The -3 dB E/O bandwidth has been extracted from Figure 11 and plotted in Figure 12-(b). A second approach is proposed by simulating the modulation bandwidth based on the carrier lifetime at z = 0 where the saturation effect is stronger. At low bias current, the first approach fits better with the experimental values. However at high electrical current (I > 80mA), the second model is more adapted.
The simulations confirmed by the measurements describe why the modulation bandwidth is limited in RSOA devices. It is mainly due to a larger carrier lifetime than in laser which is caused by a smaller photon density. The effective carrier lifetime depends on several recombination rates and strongly on the operating conditions. The stimulated recombination rate can be increased at high input optical power and electrical current. These conditions induce high photon density inside the active zone reducing the carrier lifetime and increasing the -3 dB E/O bandwidth. However these conditions are not suitable for low power consumption networks. Therefore another solution for increasing the photon density seems to be a required condition to push back the RSOA frontiers. A 3 GHz modulation bandwidth can be obtained with 850 µm long RSOA, which has led us to the first eye-opening of a RSOA at 10 Gbit/s without electrical equalization or strong optical injection. More details are presented in section 6.2.

5. System performances

The role of a RSOA as an optical transmitter is to launch a modulated optical signal into an optical fiber communication network. Reflective semiconductor optical amplifier (RSOA) devices have been developed as remote modulators for optical access networks during the past few years and their large optical bandwidth (colorless operation) has placed them in a leading position for the next generation of transmitters in WDM systems. In RSOA devices, the wavelength is externally fixed. Various options have been studied such as using multi-wavelength sources (such as tuneable lasers, External cavity laser (ECL) , Photonic Integrated Circuits (PIC) or a set of Directly Modulated Laser (DML) at selected wavelengths), creating a cavity with the active medium of the RSOA, or using filtered white source. Therefore, RSOA devices as colourless transmitters can be used in different configurations:

- Laser seeding
- Spectrum-sliced EDFA seeding
- Wavelength re-use
- Self-seeding

In the laser seeding approach, the multi-wavelength external laser source can be located at the CO (Chanclou et al., 2007) or at the remote node (de Valicourt et al., 2009). From the CO, the optical budget is limited to 25 dB and strong RBS impairments appear. These limits are overcome by locating the laser at the remote node. One laser per remote node is needed, thus raising deployment cost, control management and power consumption issues.
Another possible architecture is using spectrum-sliced EDFA seeding. An erbium-doped fibre amplifier (EDFA) is used as a broadband source of un-polarised amplified spontaneous emission and this broad spectrum is then sliced by the Arrayed Waveguide Grating (AWG) for each ONU (Healey et al., 2001).
Wavelength re-use has been developed by Korean and Japanese companies (Lee W. R. et al., 2005). The downstream source from the CO is re-modulated as an upstream signal at the

ONU using RSOA. Simple efficient ONU is obtained as no additional optical source is needed.

The final approach is using a RSOA-based self-seeding architecture. This recent concept has been proposed by Wong in 2007. This novel scheme uses at the remote node (RN) a reflective path to send back the ASE (sliced by the AWG) into the active medium. The self-seeding of the RSOA creates a several km long cavity between ONU and RN. The wavelength is determined by the connection at the RN. This technique is attractive because a self-seeded source is functionally equivalent to a tuneable laser. Recent progresses show 2.5 Gbit/s operation based on stable self-seeding of RSOA (Marazzi et al, 2011). Another way to obtain self-seeding configuration is using an external cavity laser based on a RSOA and Fiber-Bragg Grating (FBG). BER measurements show that the device can be used for upstream bit rates of 1.25 Gbit/s and 2.5 Gbit/s (Trung Le et al., 2011).

In this chapter, we focus on the laser seeding approach. We present the scheme of a laser seeding architecture based on RSOA on Figure 13. Actually, Figure 13 shows the up-stream part of the link using an RSOA, i.e. the information sent from the subscriber to operator/network. At the central office, a transmitter is used to send light (containing no information) to the subscriber through an optical circulator. Light propagates through several kilometres of optical fibre. The signal is then amplified and modulated by the RSOA in order to transmit the subscriber data for uplink transmission.

In this section, we demonstrate an extended reach hybrid PON, based on a very high gain RSOA operating at 2.5 Gbit/s. To reduce RBS impairments, we locate the continuous wave (CW) feeding light source in the remote node, and the large gain of the RSOA allows using moderate CW powers. Alternative devices such as remotely pumped erbium doped fiber amplifier (EDFA) can be used in order to avoid the deployment of active devices in a remote node; this approach could also reduce the RBS level owing to a lower seed power and the management cost of the system (Oh et al., 2007).

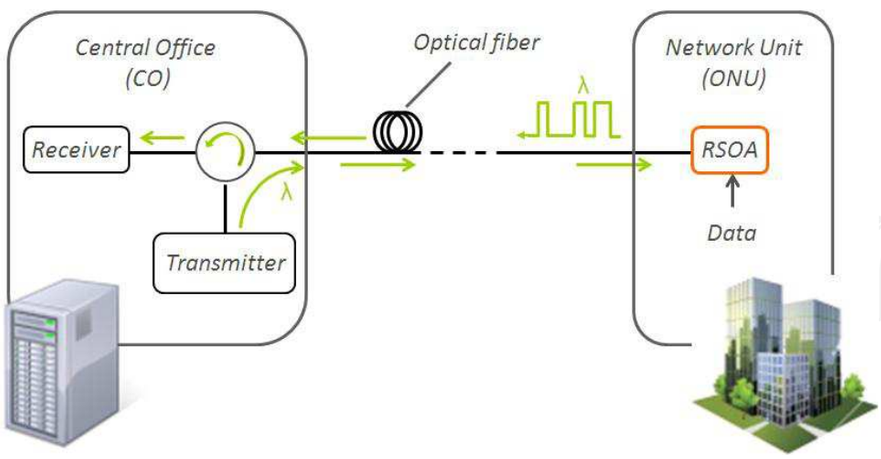

Fig. 13. Laser seeding Network architecture based on RSOA

Figure 14 shows the up-stream part of the proposed link. At the remote node, an external cavity laser (ECL) is used to launch an 8 dBm CW signal into the system through an optical circulator (OC). A wavelength demultiplexer is used to break a potential multi-wavelength signal back into individual signals. A given wavelength represents one of up to 8 sub-PON on a 100 GHz grid (from λ_1 = 1553.3 nm to λ_8 = 1558.9 nm). The output of the wavelength

demultiplexer is coupled into a 20 km long Single Mode Fibre (SMF) followed by a 12 dB optical attenuator used to simulate a passive splitter for 16 subscribers. The CW signal is then modulated by the RSOA, generating the upstream signal. The RSOA is driven by a 2^{31}-1 pseudo-random bit sequence (PRBS) at 2.5 Gbit/s, with a DC bias of 90 mA. From the remote node, the upstream signal propagates on another 25 km long SMF which simulates the reach extension provided by the proposed network design. A variable optical attenuator is placed in front of the receiver in order to analyze the performance of the system as a function of the optical budget. This attenuator also accounts for the insertion-loss of the multiplexer at the CO (between 3 to 5 dB). Bit-error-rate (BER) measurements are done using an Avalanche Photo-Diode (APD) receiver and an error analyzer.

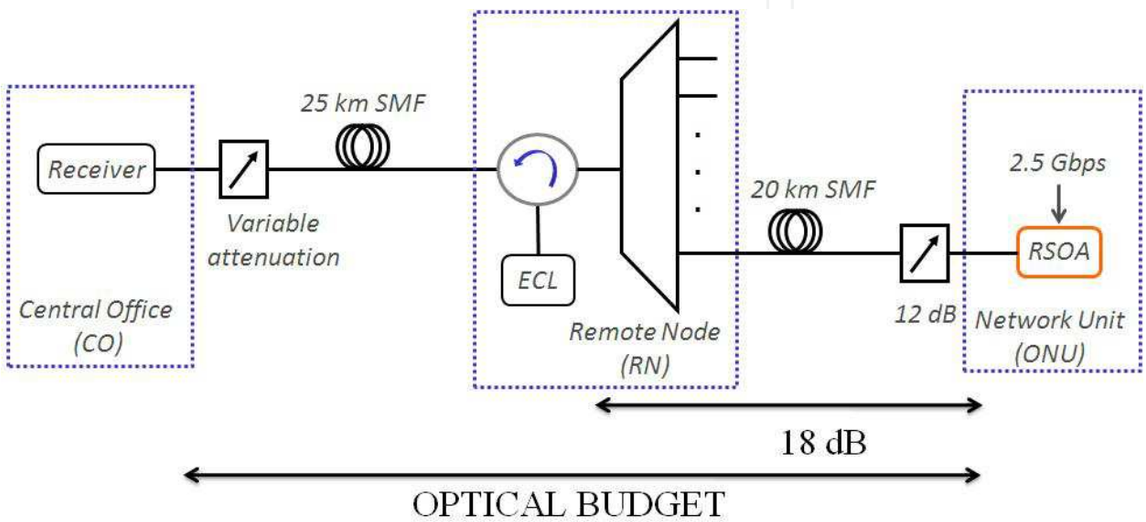

Fig. 14. Experimental setup of WDM/TDM architecture using RSOA (de Valicourt et al., 2010a)

At low bit rate, the best trade-off between gain, modulation bandwidth and saturation power is obtained for a 700 µm long cavity RSOA, therefore we chose this device in the experimental setup. The RSOA is driven at 90 mA with a -10 dBm input power. Figure 15 displays BER measurements performed at 1554.1 nm and 2.5 Gbit/s as a function of the optical budget between the CO and the extended optical network unit (ONU). The inset shows the open eye diagram measured at the output of the RSOA. Sensitivities at 10^{-9} in back-to-back (BtB) configuration and after transmission are -32 dBm and -27 dBm respectively. These performances are mainly due to the large output power of the RSOA, which allows for an increased optical budget compared to standard RSOAs: a BER of 10^{-9} is thus measured with an optical budget of more than 36 dB. Whatever the OB, the input power in the RSOA is -10dBm, which ensures that the device operates in the saturated regime, with a reflection gain of 20 dB. Gain saturation leads to a low sensitivity of the RSOA to back-reflections, since the output power only slightly depends on the input power. In Figure 15 (b), the BER of 8 WDM channels (100GHz spacing), is shown, for a 40 dB optical budget ; in this case, the BER is 10^{-7}, well below the forward error correction (FEC) limit. No penalty is observed due to the large bandwidth of the RSOA. Besides, this OB corresponds to two 12 dB (16*16 subscribers) power splitters, taking into account mux/demux, propagation and circulator losses. A compromise between split ratio and range needs to be

considered. Thus, one of the two 12 dB budget increase can also allow reach extension between the CO and the remote node (including the 25 km reach extension). However, propagation effects such as RBS and dispersion in the fibre would limit this extension. A reduction in RBS level is also needed to improve the performance of this configuration. Different solutions have been studied to reduce the RBS level such as: frequency modulation of the laser source or applying bias dithering at the RSOA.

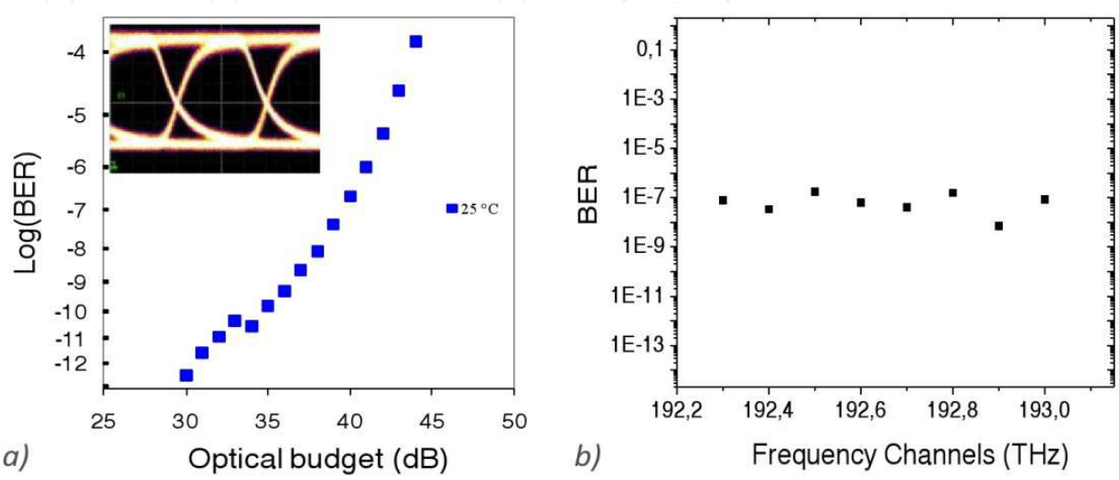

Fig. 15. (a) BER as a function of the optical budget. Inset: 2.5 Gbit/s eye-diagram at the output of the RSOA driven at 90 mA and with an input power of -10 dBm (b) BER values for different λ-channels for an optical budget of 40 dB, or a Rx input power of -30 dBm (de Valicourt et al., 2010a)

A cost effective hybrid WDM/TDM-PON which can potentially feed 2048 subscribers (16×16×8 = 2048 subscribers) at a data rate of 2.5 Gbit/s is presented in this section. The large gain and high output power of the RSOA have also allowed extending the link reach up to 45 km instead of the standard 20 km. However, these achievements are obtained at the expense of an increase in deployment and operation costs. We believe this solution is economically viable since these costs are shared between many users, and multi-wavelength sources are becoming cheaper with the advent of Photonic Integrated Circuits (PIC). This 2.5 Gbit/s upstream colourless result allows investigating this solution to achieve in the trunk line a wavelength multiplex of several next generation access solutions (10 Gbit/s down- and 2.5 Gbit/s up-stream).

6. Limitations and improvements

Architecture based on single-fibre bidirectional link seems the most interesting and cost efficient approach. ONU becomes a key element for the network evolution. Transparent and flexible architecture based on WDM technology is necessary thus colourless ONU need to be available. High gain should be provided by the transmitter to reach the necessary optical budget and high modulation speed is needed. Bit rates up to 10 Gbit/s (per wavelength) are required to follow the evolution of the 10 Gbit/s GPON. RSOA could be the missing building block to reach this ideal network. However the modulation bandwidth and the chirp are still issues that need to be solved.

6.1 Long reach PON using low chirp RSOA

Another question about Hybrid PON is its property to be compatible with long reach network configuration. It was shown in the previous section that high gain RSOAs enable high optical budget, for instance, up to 36 dB and 45km transmission at 2.5 Gbit/s. A high optical budget is necessary to obtain a long reach PON (compensation of the fibre attenuation). The limitation imposed on the bit rate and distance by the fibre dispersion can dramatically increase depending on the spectral width of the source. This problem can be overcome by reducing the chirp produced by the RSOA device. Chirp reduction was demonstrated using a 2-section RSOA and how it can be used to reduce the transmission penalties (de Valicourt et al., 2010b). We propose an extended reach hybrid PON, taking advantages of a very high gain Reflective Semiconductor Optical Amplifier (RSOA) and the two-electrode configuration operating at 2.5 Gbit/s (de Valicourt et al., 2010c).

Two RSOAs with a cavity length of 500 µm are used in the experimental setup, one with mono and the other with dual-electrode configuration. The dual-electrode RSOA was realized by proton implantation in order to separate both electrodes. The single electrode RSOA was driven at 60 mA and the dual-electrode at 20 mA on the input electrode and 115 mA at the mirror electrode. Both current values correspond to optimized conditions in order to obtain low transmission penalties. It is to be noted that in a dual-electrode RSOA, the AC current is applied to the input/output electrode. In both cases, the CW optical input power was –8.5 dBm. Fig. 16 displays BER measurements performed at 1554 nm and 2.5 Gbps as a function of the received power for one electrode and two-electrode RSOA. The penalties due to 100 km transmission with a single electrode RSOA do not enable to reach the FEC limit. From 25 km to 50 km (100 km), we obtain penalties of 1.2 (3.4) dB. One can see that a BER of 10^{-4} (FEC limit) has thus been measured with bi-electrode RSOA at a received optical power of -35 dBm over 100 km SMF. The penalties due to extended 25 and 50 km SMF are much lower than with single electrode RSOA (respectively 0.5 and 1.4 dB). These transmission

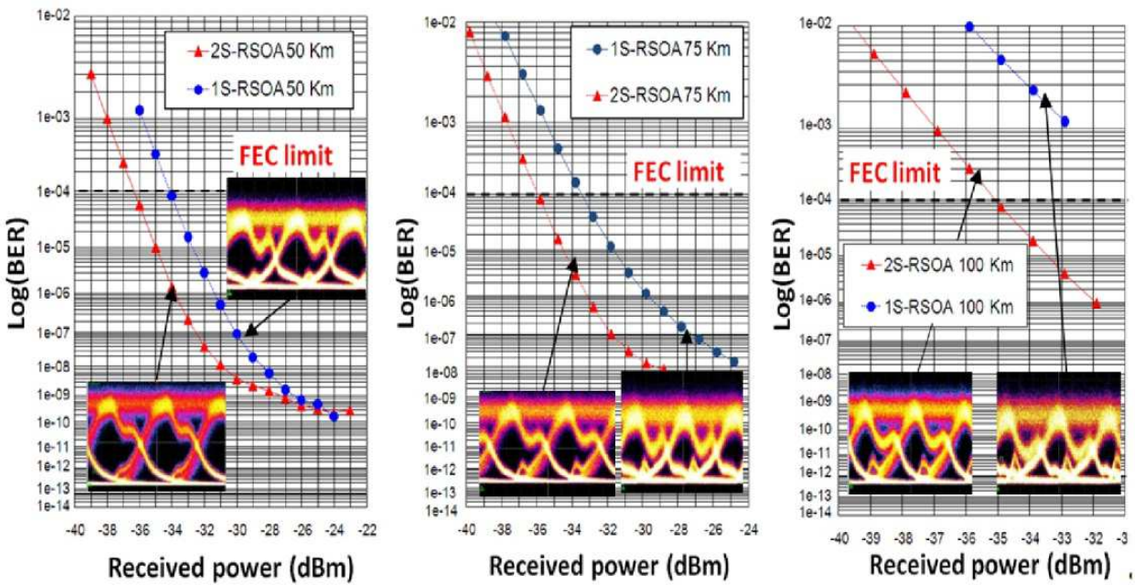

Fig. 16. Comparison of BER value as a function of the received power for mono-electrode and bi-electrode RSOA over 50, 75 and 100 km at 2.5 Gbps (de Valicourt et al., 2010c).

results clearly show the correlation between the penalty and the chirp. The latter has more pronounced effects over long SMF. In Figure 16, a comparison between single and bi-electrode RSOA over 100 km transmission is shown and a difference of 4.1 dB is obtained at the FEC limit. We can clearly see that the eye diagram starts to be closed due to the chirp on single-electrode devices over long distances. This effect is much reduced when using bi-electrode RSOAs which confirms BER measurements. The proposed network design allows the use of Dense-WDM (DWDM) which means 62 wavelengths considering the 50 nm optical bandwidth of the RSOA. By considering the passive splitter (four clients), 248 potential suscribers can be feeded. At the FEC level, a variable attenuation of 4 dB is obtained which can be use as a splitter in order to design two parallels WDM PONs (2*248=496 customers) over 100Km.
It was shown that the large gain of the RSOA and also the low chirp allows a reach extension of the link from standard 20km to 100 km. We demonstrated that penalties due to the transmission over 100 km SMF at 2.5 Gbit/s are reduced using an optimized multi-electrode device and a BER below the FEC limit was achieved. We also believe this effect will be even more pronounced when 10 Gbit/s RSOA will be used.

6.2 Reaching 10 Gbit/s modulation without any electronic processing

Active research on high bit rate RSOA has led to 10 Gbit/s operation with EDC (Torrientes et al., 2010), OFDM (Duong et al., 2008) or electronic filtering (Schrenk et al, 2010). Bandwidth improvement to 7 GHz small-signal bandwidth with dual-electrode devices have been obtained but no large signal operation (Brenot et al, 2007). However the modulation bandwidth of one-section RSOA is limited to 2 GHz and increasing the modulation bandwidth of RSOA is still a challenge. Since carrier lifetime is mainly governed by stimulated emission rate, we have decided to increase the length of our RSOA to increase photon density, hence reducing carrier lifetime (de Valicourt et al., 2011). This device was chosen because an open eye diagram was obtained when the RSOA was driven by a 2^7-1 PRBS at 10 Gbit/s (Figure 17. (a)). The experimental set-up used for the 10 Gbit/s modulation is the same as represented in Figure 13. An ECL is used to launch a 4.5 dBm CW signal into the system through an optical circulator (OC). The signal is coupled into the RSOA which is modulated and generates the upstream signal. The RSOA is driven by a 2^7-1 PRBS at 10 Gbit/s, with a DC bias of 160 mA. The upstream signal propagates on various SMF lengths. A variable optical attenuator is placed in front of the receiver in order to analyze the performance of the system as a function of the received power. BER measurements are done using an APD receiver and an error analyzer. BER measurements without ECL have led to a BER floor of 10^{-6} (ASE regime).
With optical injection, BER values below the FEC limit in BtB and after 2km transmission are obtained (Figure 17. (b)). Error-free operation can either be obtained with FEC codes, or under certain optical injection regimes. However we can clearly see that the eye diagram tends to be closed due to the chirp over long distances. Multi-electrode devices can be used in order to compensate for this effect as demonstrated in the previous section.
As described in section 4, the modulation speed of RSOA is limited by the carrier lifetime. In the large signal regime, the slow decay is probably governed by the no-stimulated recombination process, which increases the carrier lifetime. A 3 GHz modulation bandwidth can be obtained with 850 μm long RSOA, which has led to the first eye-opening of a RSOA at 10 Gbit/s without electrical equalization or passive electronic filtering. Limitation due to

the chirp is observed and further works are underway to overcome this effect using multi-electrodes devices. Longer devices and dual-electrode devices will be studied to improve the modulation and transmission properties.

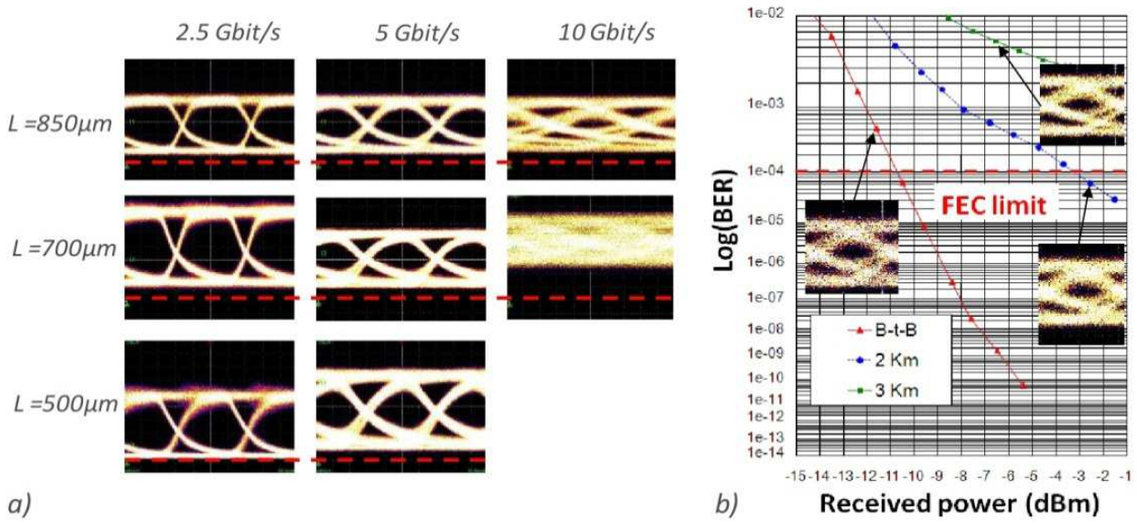

Fig. 17. (a) Eye diagrams at various bit rates of RSOA whose length varies from 500 to 850 µm. The collected power is pure ASE. Red lines are the dark levels. (b) BER value as a function of the received power for 850 µm long RSOA modulated at 10 Gbit/s (de Valicourt et al., 2011)

7. Conclusion

Nowadays, research in the telecom area is partly focused on passive optical network architecture. WDM-PON seems to be a promising approach allowing high data bit rate and flexibility. WDM techniques used in long-haul systems are now mature, however the shift to local access networks is more challenging. New requirements appear such as cost reduction, the need for new key devices at the ONU and compatibility with the existing network. Colourless ONU are necessary to obtain cost effective architecture and RSOA is one potential solution. In this chapter, we focused on these devices.

The SOA theory has been discussed and applied to Reflective SOA devices. We underline several physical mechanisms that are responsible for the carrier density variation. The stimulated, radiative and non-radiative recombination rates are described. A model has been developed, taking into account several longitudinal sub-sections of the active guide. RSOAs exhibit a non-homogeneous carrier density profile which strongly affects the overall gain. At the input/output of the device, a strong saturation effect is observed. Therefore the net gain needs to be carefully integrated along the device taking in account this non-homogeneity. All these results confirm the presence of key parameters such as the length and the optical confinement which should lead to design rules.

To assess the RSOA dynamics, the carrier lifetime is estimated. The E/O modulation bandwidth mainly depends on this parameter, for instance shorter carrier lifetime induces larger 3 dB E/O modulation bandwidth. The reduction of the carrier lifetime is required to obtain high speed RSOAs.

Potential cost effective solutions for next generation of access network could be based on RSOA devices. Therefore, research on RSOA devices is driven by WDM-PON applications. It is of prime interest to solve issues related to this application. RSOAs as colourless ONU have been investigated for access network. High performances RSOAs enable an upstream transmission of 8 WDM channel at 2.5 Gbit/s over 45 km. A high optical budget (36 dB) was demonstrated.

The chirp remains one major limiting factor as well as the modulation speed. 2-section RSOAs were used to overcome the first drawback. The use of 2-section RSOAs allows a 100 km transmission below the FEC limit at 2.5 Gbit/s. Finally, long RSOA allows performing the first direct 10 Gbit/s modulation with open eye diagram thanks to the E/O modulation bandwidth increase.

Therefore, as a general conclusion, RSOAs show a great potential as a next generation of optical transmitter. It is a colorless device which can be used in WDM access networks. However the modulation speed is still limited and 10 Gbit/s modulation needs to be realised over a minimum of ten kilometres.

Tech-eco analysis has to be performed in order to evaluate the different technologies for WDM-PON and a trade-off between performances and cost will determine the future of optical access network. RSOA are still limited in terms of performances and architecture but new approach such as self-seeding could overcome these main issues.

8. Acknowledgements

The work in this chapter would not have been possible without the support of numerous people and I would like to acknowledge a few of them here. Firstly, the author would like to thank Dr. Romain Brenot for his guidance and advices.

Next I would like to thank fellow workers at III-V lab, especially Francis Poingt and Marco Lamponi who worked closely with me. This collaboration was key to the success of this study. Additionally, I wish to acknowledge Dr. Philippe Chanclou for the fruitful discussions.

9. References

An F.T, Soo Kim K., Gutierrez D., Yam S., Hu E., Shrikhande K., & Kazovsky L.G. (2004),"SUCCESS: A Next-Generation Hybrid WDM/TDM Optical Access Network Architecture", *J. Lightwave Technol.*, Vol. 22, No. 11, November 2004

Brenot R., Pommereau F., Le Gouezigou O., Landreau J., Poingt F., Le Gouezigou L., Rousseau B., Lelarge F., Martin F., & Duan G-H (2005), "Experimental study of the impact of optical confinement on saturation effects in SOA", *in proc. OFC 2005*, OME50, March 2005

Brenot R., Provost J.-G., Legouezigou O., Landreau J., Pommereau F., Poingt F., Legouezigou L., Derouin E., Drisse O., Rousseau B., Martin F., Lelarge F., & Duan G.H. (2007), "High modulation bandwidth reflective SOA for optical access networks", *in Proc. ECOC*, 2007, pp. 1-2, Berlin, Germany

Buldawoo N., Mottet S., Le Gall F., Sigonge D., Meichenin D., & Chelles S. (1997), "A Semiconductor Laser Amplifier-Reflector for the future FTTH Applications", *in Proc. ECOC'97*, Sept. 1997, pp. 196-199, Edinburgh, UK

Chanclou P., Payoux F., Soret T., Genay N., Brenot R., Blache F., Goix M., Landreau J., Legouezigou O., & Mallécot F. (2007), "Demonstration of RSOA-based remote

modulation at 2.5 and 5 Gbit/s for WDM PON", *in Proc. OFC*, OWD1, 2007, Anaheim, USA

Connelly M. J., "Wide-Band Steady-State Numerical Model and Parameter Extraction of a Tensile-Strained Bulk Semiconductor Optical Amplifier," *IEEE J. Quantum Electroni.*, Vol. 43, No. 1, Jan. 2007, pp. 47-56

D'Alessandro D., Giuliani G., & Donati S. (2001), "Spectral gain and noise evaluation of SOA and SOA-based switch matrix", *IEE Proc.-Optoelectron.*, Vol. 148, No. 3, June 2011, pp. 125-130

de Valicourt G., Maké D., Fortin C., Enard A., Van Dijk F., & Brenot R. (2011), "10Gbit/s modulation of Reflective SOA without any electronic processing", *in Proc. OFC'11*, OThT2, 2011, Los Angeles, USA

de Valicourt G., Make D., Lamponi M., Duan G., Chanclou P. , & Brenot R. (2010a), "High Gain (30 dB) and High Saturation Power (11dBm) RSOA Devices as Colourless ONU Sources in Long Reach Hybrid WDM/TDM -PON Architecture", *Photonics technology letters*, Vol. 22, No. 3, Feb. 2010, pp. 191-193

de Valicourt G., Pommereau F., Poingt F., Lamponi M., Duan G.H., Chanclou P., Violas M. A., & Brenot R. (2010b) "Chirp Reduction in Directly Modulated Multielectrode RSOA Devices in Passive Optical Networks", *Photonics technology letters*, Vol. 22, No. 19, Oct. 1, 2010, pp. 1425-1427

de Valicourt G., Lamponi M., Duan G.H., Poingt F., Faugeron M., Chanclou P., & Brenot R. (2010c), " First 100 km uplink transmission at 2.5 Gbit/s for hybrid WDM/TDM PON based on optimized bi-electrode RSOA", *in Proc. ECOC'10*, Tu.5.B.6, 2010, Torino, Italy

de Valicourt G., Maké D., Landreau J., Lamponi M., Duan G.H., Chanclou P. , & Brenot R. (2009), "New RSOA Devices for Extended Reach and High Capacity Hybrid TDM/WDM -PON Networks", *in Proc. ECOC'09*, P9.5.2, 2009, Vienna, Austria

Duong T., Genay N., Chanclou P., Charbonnier B., Pizzinat A., & Brenot R., "Experimental demonstration of 10 Gbit/s upstream transmission by remote modulation of 1 GHz RSOA using adaptively modulated optical OFDM for WDM-PON single fiber architecture," *in Proc. ECOC*, Th.3.F, Sep. 2008, Brussels, Belgium

Feuer M., Wiesenfeld J., Perino J., Burrus C., Raybon G., Shunk S., & Dutta N. (1996), "Single-port laser-amplifier modulators for local access", *Photonics technology letters*, Vol.8, No.9, Sept. 1996, pp.1175-1177

Healey P., Townsend P., Ford C., Johnston L., Townley P., Lealman I., Rivers L., Perrin S. , & Moore R. (2001), "Spectral slicing WDM-PON using wavelength-seeded reflective SOAs", *Electron. Lett.*, Vol. 37, No. 19, Sept. 2001, pp. 1181 – 1182

Iezekiel S., Elamaran B., & Pollard R.D. (2000), "Recent developments in lightwave network analysis", *Engineering Science and Education Journal*, Vol. 09, No. 06, Dec. 2000, pp. 247-257

Kao K. C. & Hockham G. A. (1996), Dielectric-fibre surface waveguides for optical frequencies, *Proc. IEE*, Vol. 113, No. 7, July 1966, pp. 1151-1158

Koponen J.J., & Söderlund M.J. (2004), "A duplex WDM passive optical network with 1:16 power split using reflective SOA remodulator at ONU", *in proc. OFC'04*, MF 99, March 2004, Los Angeles, USA

Lee H-H., Cho S-H., Lee J-H., Jung E-S., Yu J-H., Kim B-W., Lee S-S., Lee S-H., Koh B-H., Sung J-S., Kang S-J., Kim J-H., & Jeong K-T. (2009), "First Commercial Service of a Colorless Gigabit WDM/TDM Hybrid PON System", *in Proc. OFC*, PDPD9, 2009, San Diego, USA

Lee W. R., Park M. Y., Cho S. H., Lee J. H., Kim C. Y., Jeong G., & Kim B. W. (2005), "Bidirectional WDM-PON based on gain-saturated reflective semiconductor optical amplifiers", *Photonics technology letters*, Vol. 17, No. 11, Nov. 2005, pp. 2460–2462

Lelarge F., Chimot N., Rousseau B., Martin F., Brenot R., & Accard A. (2010), "Chirp Optimization Of 1550 nm InAs/InP Quantum Dash Based Directly Modulated Lasers For 10Gb/s SMF Transmission Up To 65Km" *in proc. IPRM*, May-June, 2010, pp. 1-3, Kagawa, Japan

Liu Z., Sadeghi M., de Valicourt G., Brenot R., & Violas M.(2011), "Experimental Validation of a Reflective Semiconductor Optical Amplifier Model used as a Modulator in Radio over Fiber Systems", *Photonics technology letters*, Vol. 23, No. 9, May 1, 2011, pp. 576-578

Marazzi L., Parolari P., de Valicourt G., & Martinelli M. (2011), "Network-Embedded Self-Tuning Cavity for WDM-PON Transmitter", *in proc. ECOC*, Mo.2.C.3, Sept. 2011, Geneva, Switzerland

Oh J., Koo S. G., Lee D., & Park S-J. (2007), "Enhanced System Performance of an RSOA Based Hybrid WDM/TDM-PON System Using a remotely Pumped Erbium-Doped Fiber Amplifier", *in Proc. OFC*, PDP9, 2007, Anaheim, USA

Olshansky R., Su C. A., Manning J., & Powazinik W. (1984), "Measurement of radiative and nonradiative recombination rates in InGaAsP and AlGaAs light sources", *J. Quantum Electron.*, Vol. 20, No. 8, 1984, pp. 838-854

Olsson N. A. (1988), "Polarisation-independent configuration optical amplifier", *Electron. Lett.*, Vol. 24, No. 17, Aug. 1988, pp. 1075-1076

Omella M., Polo V., Lazaro J., Schrenk B., & Prat J. (2008), "10 Gb/s RSOA Transmission by Direct Duobinary Modulation", *in Proc. ECOC'08*, Tu.3.E.4, Sept. 2008, Brussels, Belgium

Otani T., Goto K., Abe H., Tanaka M., Yamamoto H., & Wakabayashi H. (1995), "5.3 Gbit/s 11300 km data transmission using actual submarine cables and repeaters", *Electron. Lett.*, Vol. 31, No. 5, 1995, pp. 380-381

Prat J., Arellano C., Polo V., & Bock C. (2005), "Optical network unit based on a bidirectional reflective semiconductor optical amplifier for fiber-to-the-home networks", *Photonics technology letters*, Vol.17, No.1, January 2005, pp.250-252

Schrenk B., de Valicourt G., Omella M., Lazaro J., Brenot R., & Prat J. (2010), "Direct 10 Gb/s Modulation of a Single-Section RSOA in PONs with High Optical Budget", *Photonics technology letters*, Vol. 22, No. 6, March 15, 2010, pp. 392-394

Tanaka S., Tomabechi S., Uetake A., Ekama M., & Morito K. (2006), Recard high saturation output power (+20 dBm) and Low NF (6.0 dB) polarization-insensitive MQW-SOA module, *IET Electronics Letters*, Vol. 42, No. 18, August 2006, pp. 1050-1060

Torrientes D., Chanclou, P., Laurent F., Tsyier S., Chang Y., Charbonnier B., & Raharimanitra F. (2010), RSOA-Based 10.3 Gbit/s WDM-PON with Pre-Amplification and Electronic Equalization, *in proc. OFC*, JThA28, 2010, San Diego, USA

Trung Le Q., Deniel Q., Saliou F., de Valicourt G., Brenot R., & Chanclou P. (2011), RSOA-based External Cavity Laser as Cost-effective Upstream Transmitter for WDM Passive Optical Network, *CLEO 2011*, JWA9, May 1-6, 2011, Baltimore, USA

Wong, E., Ka Lun Lee, & Anderson T.B. (2007), Directly Modulated Self-Seeding Reflective Semiconductor Optical Amplifiers as Colorless Transmitters in Wavelength Division Multiplexed Passive Optical Networks, *J. Lightwave Technol.*, Vol. 25, No. 1, January 2007

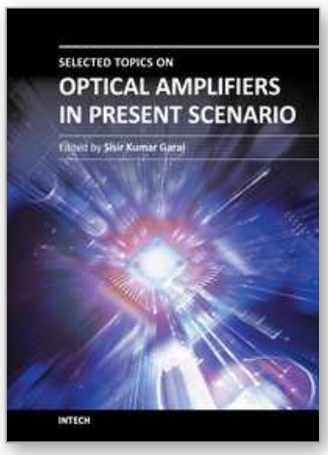

Selected Topics on Optical Amplifiers in Present Scenario

Edited by Dr. Sisir Garai

ISBN 978-953-51-0391-2

Hard cover, 176 pages

Publisher InTech

Published online 23, March, 2012

Published in print edition March, 2012

With the explosion of information traffic, the role of optics becomes very significant to fulfill the demand of super fast computing and data processing and the role of optical amplifier is indispensable in optical communication field. This book covers different advance functionalities of optical amplifiers and their emerging applications such as the role of SOA in the next generation of optical access network, high speed switches, frequency encoded all-optical logic processors, optical packet switching architectures, microwave photonic system, etc. Technology of improving the gain and noise figure of EDFA and, the study of the variation of material gain of QD structure are also included. All the selected topics are very interesting, well organized and hope it will be of great value to the postgraduate students, academics and anyone seeking to understand the trends of optical amplifiers in present scenario.

InTech Europe

University Campus STeP Ri
Slavka Krautzeka 83/A
51000 Rijeka, Croatia
Phone: +385 (51) 770 447
Fax: +385 (51) 686 166
www.intechopen.com

InTech China

Unit 405, Office Block, Hotel Equatorial Shanghai
No.65, Yan An Road (West), Shanghai, 200040, China
中国上海市延安西路65号上海国际贵都大饭店办公楼405单元
Phone: +86-21-62489820
Fax: +86-21-62489821

IntechOpen